J Mater Sci (2011) 46:1680–1684
DOI 10.1007/s10853-010-4985-3

Effect of heating rate on the microstructural and magnetic properties of nanocrystalline $Fe_{81}Si_4B_{12}P_2Cu_1$ alloys

M. Guo · Y. G. Wang · X. F. Miao

Received: 12 August 2010 / Accepted: 5 October 2010 / Published online: 20 October 2010
© Springer Science+Business Media, LLC 2010

Abstract The effect of heating rate on the structural and magnetic properties of the nanocrystalline $Fe_{81}Si_4B_{12}P_2Cu_1$ alloy has been investigated. Amorphous $Fe_{81}Si_4B_{12}P_2Cu_1$ alloy was annealed at 753 K for 180 s at different heating rates ranging from 0.05 to 5 K/s in protective argon atmosphere. The structural and magnetic properties of the as-quenched and annealed alloys were studied using X-ray diffractometer (XRD), differential scanning calorimeter (DSC), vibrating sample magnetometer (VSM), and B–H loop tracer, respectively. Amorphous precursor prepared by industry-grade raw materials is obtained. The increase of heating rate is found to be significantly effective in decreasing the grain size of α-Fe(Si) phase, but the grain size increases at higher heating rate. The volume fraction of α-Fe(Si) phase shows a monotonic decrease with the increase of the heating rate. The coercivity H_c markedly decreases with increasing heating rate and exhibits a minimum at the heating rate of 0.5 K/s, while the saturation magnetization, M_s, shows a slight decrease. These results suggest that the effect of heating rate on H_c and M_s is originated from the changes of grain size and the volume fraction of α-Fe(Si) phase.

Introduction

Nanocrystalline alloys have been extensively studied because of their promising technological applications [1–4]. Considerable attention is devoted to the Fe-based soft magnetic nanocrystalline materials such as Finemet-type nanocrystalline alloys [1], Nanoperm-type nanocrystalline alloys [5], and Hitperm-type nanocrystalline alloys [6], which show excellent soft magnetic properties: high-saturation magnetic induction like Fe-based metallic glasses, high permeability like cobalt-based metallic glasses [7], and high electrical resistivity leading to low eddy current losses, making these materials useful for various soft magnetic applications [8–10]. Recently, Makino et al. [11–13] reported FeSiBCuP nanocrystalline soft magnetic alloys with higher B_s of around 1.88–1.94 T. The simultaneous addition of P and Cu drastically decreases the grain size originating from the mixing enthalpy [ΔH] between the constituent elements, and the elimination of transition metals such as Nb is helpful not only to reduce costs but also to produce the alloys in air.

Alloys with a microstructure of small nanocrystallites (10–20 nm) embedded in amorphous matrix are usually obtained by annealing the as-quenched amorphous [8, 14–16] alloys above their crystallization temperature. The improvement of the soft magnetic properties for various nanocrystalline alloys strongly depends on the average grain size, D, which gives rise to the significant decrease of the effective magnetic anisotropy [17] and a suitable volume fraction of α-Fe(Si) nanocrystallites in the materials which results in the compensation of the net magnetostriction of two phases (positive magnetostriction of the amorphous phase and negative magnetostriction of the nanocrystalline α-Fe(Si) phase) [18]. The average grain size, D, and the volume fraction of nanocrystallites, V_{cr}, vary significantly with the annealing conditions [14, 19, 20]. Studying the effect of annealing conditions on the structure of the alloy is helpful not only to realize the origin of excellent soft magnetic properties but also to optimize the heat-treatment conditions. In the present

M. Guo · Y. G. Wang (✉) · X. F. Miao
College of Materials Science and Technology, Nanjing University of Aeronautics and Astronautics, Nanjing 210016, People's Republic of China
e-mail: yingang.wang@nuaa.edu.cn

work, we report the heating rate dependence of microstructural and magnetic properties of FeSiBCuP-type alloy composed of a nanocrystalline phase in an amorphous matrix. For the economical and functional purpose, the ribbon was prepared from industry-grade raw materials, which will not limit its potential large-scale applications caused by the high cost of purity materials.

Experimental

Alloy ingots of nominal composition $Fe_{81}Si_4B_{12}P_2Cu_1$ were produced by arc-melting of industry-grade raw materials: Fe, Fe–B, Fe–P, Cu, and Si in high purity argon atmosphere.

The rapidly solidified ribbons (typical dimension of about 20 μm thick and 1.2 mm wide) were prepared by a single-roller melt-spinning method at a wheel speed of 40 m/s under purity argon atmosphere. The cooling rate was high enough to ensure amorphous state in the ribbons. The nanocrystalline alloys composed of a nanocrystalline phase embedded in an amorphous matrix were obtained by annealing the as-quenched amorphous ribbons in suitable heat-treatment conditions.

The structures of the as-quenched and the annealed ribbons were examined by XRD using Cu Kα_1 radiation. The mean grain size, D, of the α-Fe(Si) phase was evaluated by using the Scherrer formula from the full width at half maximum of the bcc (110) X-ray diffraction peak. Differential scanning calorimeter (DSC) measurement with increasing temperature at a heating rate of 25 K/min in N_2 atmosphere was used to find out a proper annealing regime for the as-quenched amorphous ribbon sample. The as-spun sample was heat treated at 753 K for 180 s in protective argon atmosphere with heating rates from 0.05 to 5 K/s, and then quickly cooled to room temperature. B–H loop tracer and vibrating sample magnetometer (VSM) were used to measure the hysteresis loops of the as-cast and thermally annealed samples in order to obtain coercive field (H_c) and saturation magnetization (M_s), respectively. All the magnetic measurements were carried out at room temperature.

Results and discussion

Microstructure and thermal properties of the as-quenched alloy

Figure 1 shows the representative XRD pattern of $Fe_{81}Si_4B_{12}P_2Cu_1$ alloy in its as-quenched state. Only one broad peak around $2\theta = 45°$ is exhibited, which is known as a diffuse halo. No peaks corresponding to the presence of crystalline phases are observed. This indicates that a single amorphous phase is formed in as-quenched ribbon.

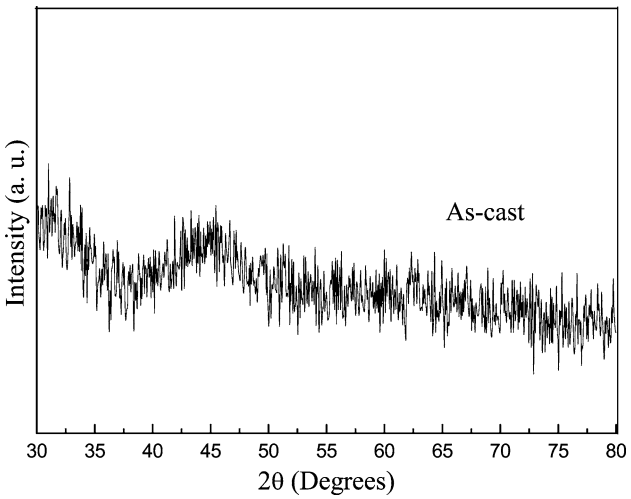

Fig. 1 XRD pattern of the $Fe_{81}Si_4B_{12}P_2Cu_1$ amorphous alloy

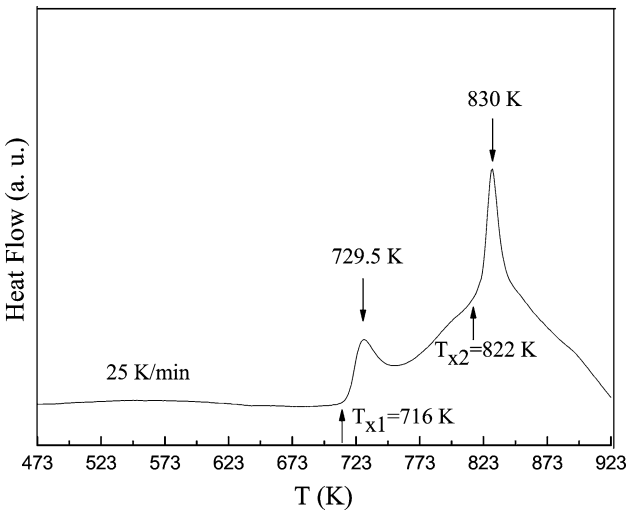

Fig. 2 DSC curve of $Fe_{81}Si_4B_{12}P_2Cu_1$ alloy, obtained at a heating rate of 25 K/min in N_2 atmosphere

Thermal analysis was carried out with a differential scanning calorimeter in N_2 flow at 25 K/min up to 973 K, which is used to evaluate the crystallization of an amorphous ribbon. The typical DSC curve is plotted in Fig. 2. Two exothermic peaks corresponding to the different crystallization events are detected during heating process with an interval of 100.5 K between them. The first and the second exothermic peaks are associated to the primary crystallization of the nanocrystalline phase from amorphous phase and to the transformation from α-Fe(Si) to FeB compounds, respectively. According to the DSC result, as-cast amorphous alloy was annealed at 753 K for 180 s in protective argon atmosphere with different heating

rates to achieve the nanocrystalline materials with α-Fe(Si) phase and free from FeB compounds.

Microstructural analysis of crystallized alloys from hetero-amorphous phase

Figure 3 shows the XRD patterns for the $Fe_{81}Si_4B_{12}P_2Cu_1$ alloy annealed at five different heating rates 0.05, 0.1, 0.5, 3, and 5 K/s, respectively. A sharp diffraction peak at about 45° corresponding to the precipitation of α-Fe(Si) appears for all the annealed samples. No other phases existed, such as the FeB phase.

The heating rate dependence of the lattice parameter *a* for annealed samples, obtained by analyzing XRD patterns, is shown in Fig. 4a. The lattice parameter varies between 0.2812 and 0.2834 nm. It should be noted that the lattice parameter is smaller than that of Fe (0.286 nm) [8]. This results from the fact that a small amount of silicon atoms substitute iron atoms in the nanocrystals, existing as Fe_3Si phase with a DO_3 structure [14]. As the heating rate increases from 0.05 to 5 K/s, the lattice constant slightly increases from 0.2812 to 0.2834 nm, suggesting that increasing heating rate decreases the concentration of Si in the α-Fe(Si) phase. This may originate from the shorter time for Si diffusing into α-Fe(Si) nanocrystallites at higher heating rates.

In Fig. 4b, the heating rate dependence of the average grain size *D* of α-Fe(Si) is shown, which determined from the sharp diffraction peak, according to the Scherrer equation [21]:

$$D = \frac{0.9\lambda}{B\cos(\theta)} \quad (1)$$

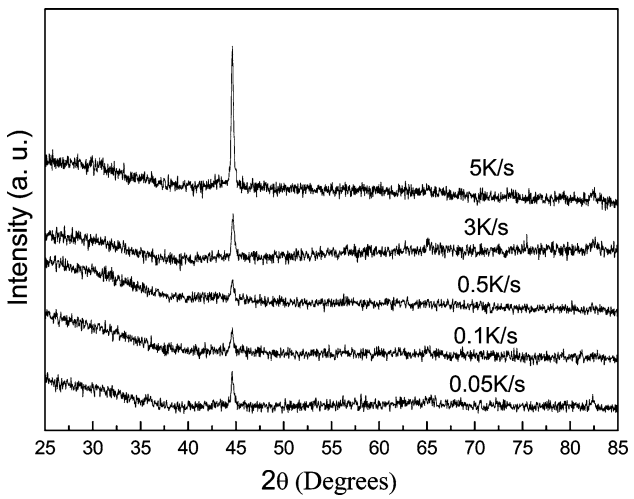

Fig. 3 Representative XRD patterns showing heating rate dependence of the crystalline phase for the samples annealed at 753 K for 180 s

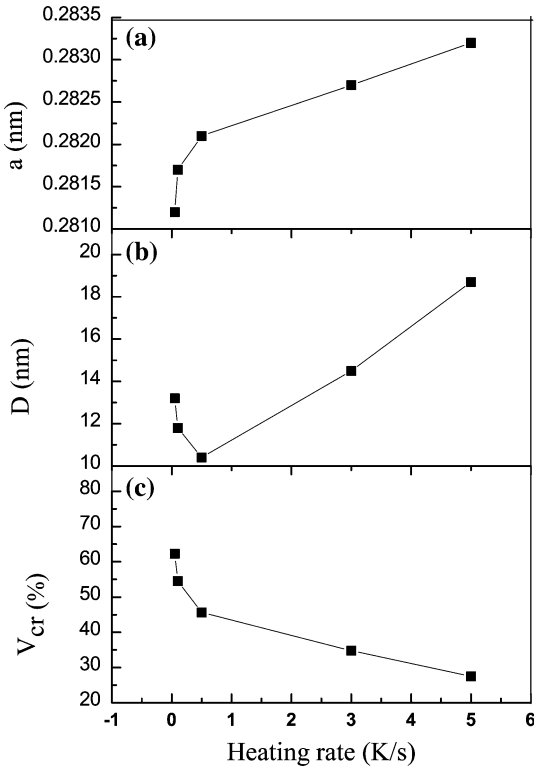

Fig. 4 Heating rate dependence of **a** the lattice parameter α, **b** the grain size *D*, and **c** the volume fraction of the nanograins V_{cr} for annealed $Fe_{81}Si_4B_{12}P_2Cu_1$ alloys. The lines are guide for the eye

where λ is the wave length of incident X-ray (λ = 1.5418 Å), *B* is the full width at half maximum of the diffraction peak, θ is the diffraction angle. The average grain size of α-Fe phases ranges from 10 to 19 nm. It is clear that the grain size comes up to a minimum value of 10.4 nm at a heating rate of 0.5 K/s. An abrupt increase of grain size is noticed at higher heating rate.

Figure 4c shows the heating rate dependence of the volume fraction of the nanograins, V_{cr}, which varies between 27% and 63%. The crystalline volume fraction V_{cr} was calculated according to the equation:

$$V_{cr} = \frac{I_{cr}}{I_{cr} + I_{am}} \quad (2)$$

where I_{cr} and I_{am} are the integral intensities of diffraction peaks of crystalline phase and amorphous phase determined from peak areas [22–24], respectively. One can see that the crystalline volume fraction decreases with increasing heating rate.

The addition of Cu is well known to be much effective in refining the grain size, because the Cu cluster forms prior to the primary crystallization of α-Fe(Si) phase during the crystallization of some kinds of Fe-based amorphous alloys, which acts as the nucleation sites for the α-Fe grains and decreases α-Fe grain size in crystallized structures

[25, 26]. During the annealing process, extremely small regions with enriched Cu and P could be formed in the FeSiBCuP amorphous alloy because of repulsive and attractive interactions existing between Fe and Cu, and Cu and P atoms, respectively [12, 27]. The number of the region is possibly large enough to be high density dispersing in the amorphous matrix, which acts as the heterogeneous nucleation sites for α-Fe(Si) and leads to the refinement of the grain. In addition, the formed Cu–P clusters can act as a diffusion barrier and will hence inhibit α-Fe(Si) grain growth. The grain size and volume fraction of α-Fe(Si) nanocrystallites are intimately correlated with the density of the Cu–P enriched clusters. With increasing the heating rate, the grain size, D, at first decreases due to the limited time for grain growth. However, increasing the heating rate during the annealing process restricts the diffusion of Cu and P elements, which results in a very low Cu- and P-enriched clusters. Consequently, high heating rate during the annealing process of $Fe_{81}Si_4B_{12}P_2Cu_1$ nanocrystalline alloys reduces the number of nucleation sites and leads to the decrease of the volume fraction and the increase of the grain size.

Magnetic characterization

The heating rate dependence of coercivity, H_c, and saturation magnetization, M_s, for the melt-spun $Fe_{81}Si_4B_{12}P_2Cu_1$ alloy annealed at 753 K for 180 s is shown in Fig. 5. As the heating rate increases, the coercivity initially decreases down to a minimum of 7.2 A/m at the heating rate of 0.5 K/s and then increases. The saturation magnetization, M_s, decreases with the heating rate increasing from 0.05 to 5 K/s.

The similarity of the heating rate dependence of the coercivity H_c and that of the grain size D implicates that the effect of heating rate on H_c originates from its effect

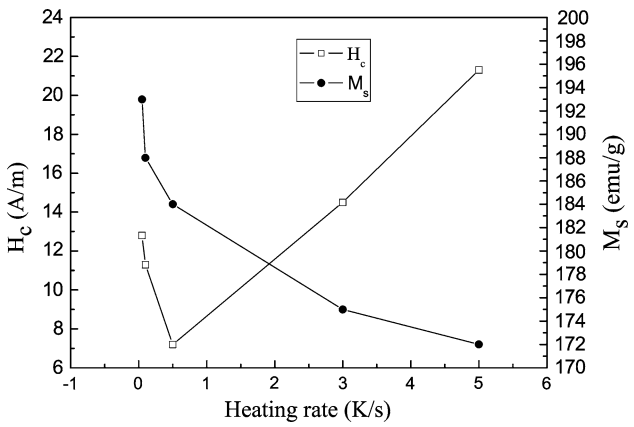

Fig. 5 Heating rate dependence of the coercivity H_c and the saturation magnetization M_s. The lines are guide for the eye

the grain size. The excellent soft magnetic properties strongly depend on the grain diameter of the nanocrystalline and the volume fraction of the α-Fe(Si) phase for the nanocrystalline soft magnetic FeSiBCuP alloys. Since the size of nanocrystallites is smaller than the ferromagnetic exchange interaction length, magnetic exchange coupling between the nanocrystalline grains through the remaining ferromagnetic amorphous phase matrix leads to the averaging out of the magnetocrystalline anisotropy [17]. The initial decrease of coercive field can be attributed to the refinement of α-Fe(Si) crystallites and the uniformity structure of α-Fe(Si) crystallites embedded in a residual amorphous matrix. The increase of coercive field at higher heating rate can be attributed to the growth of the nanograins, which reduces the exchange coupling between the nanograins.

The saturation magnetic flux density, B_s, is deeply affected by the volume fraction of the crystalline phase, V_{cr},

$$B_s = B_{sc}V_{cr} + B_{sa}(1 - V_{cr}). \quad (3)$$

The B_{sc} and B_{sa} are the saturation magnetic flux density in the crystalline and amorphous phases. The decrease of the volume fraction of the crystalline phase, V_{cr}, results in the decrease of saturation magnetization, M_s, which agrees well with the fact that the heating rate dependence of M_s is similar to that of V_{cr}.

Conclusions

The effect of heating rate on structural and magnetic properties for the $Fe_{81}Si_4B_{12}P_2Cu_1$ nanocystalline alloys has been investigated. The $Fe_{81}Si_4B_{12}P_2Cu_1$ amorphous alloy is obtained from industry-grade raw materials. The $Fe_{81}Si_4B_{12}P_2Cu_1$ alloy annealed at 753 K for 180 s with various heating rates has a structure composed of an amorphous phase and α-Fe(Si) grains with 10–19 nm in size. With the increase of the heating rate, the grain size first decreases and then increases, while the volume fraction of α-Fe(Si) phase decreases. The increase of the grain size with the heating rate is attributed to the decrease of the density of Cu- and P-enriched clusters serving as heterogeneous nucleation sites for α-Fe(Si) primary crystals. With the increase of the heating rate, H_c shows a remarkable decrease because of the reduction of the grain size, and arrives a minimum at the heating rate of around 0.5 K/s, while M_s shows a slight variation because of the change of the volume fraction of α-Fe(Si) phase. Optimum soft magnetic properties were obtained for the $Fe_{81}Si_4B_{12}P_2Cu_1$ nanocrystalline alloy ribbon annealed at 753 K for 180 s with the heating rate of 0.5 K/s, exhibiting a low H_c of 7.2 A/m and a high M_s of 184 emu/g.

References

1. Yoshizawa Y, Oguma S, Yamauchi K (1988) J Appl Phys 64:6044
2. Yoshizawa Y (1999) Mater Sci Forum 307:51
3. Peng K, Zhou LP, Hu AP, Zhu JJ, Li DY (2008) Trans Nonferrous Met Soc China 18:852
4. Chen YM, Ohkubo T, Ohta M, Yoshizawa Y, Hono K (2009) Acta Mater 57:4463
5. Suzuki K, Kataoka N, Inoue A (1990) Mater Trans JIM 31:743
6. Willard MA, Laughlin DE, McHenry ME (1998) J Appl Phys 84:6773
7. Wang Z, He KY, He SL, Zhang YM, Fu YJ, Zhang L (1997) J Magn Magn Mater 171:300
8. Modaka SS, Ghodke N, Mazaleyrat F, Bue ML, Vargad LK, Guptab A, Kane SN (2008) J Magn Magn Mater 320:828
9. Varga LK (2007) J Magn Magn Mater 316:442
10. Phan MH, Peng HX, Wisnom MR, Yu SC, Chau N (2006) Composites A 37:191
11. Makino A, Men H, Yubuta K, Kubotal T (2009) J Appl Phys 105:013922-1
12. Makino A, Men H, Kubota T, Yubuta K, Inoue A (2009) J Appl Phys 105:07A308-1
13. Makino A, Men H, Kubota T, Yubuta K, Inoue A (2009) Mater Trans JIM 50:204
14. Shahri F, Beitollahi A, Shabestari SG, Kamali S (2007) Phys Rev B 76:024434-1
15. Mini DM, Gavrilovi A, Angererb P, Mini DG, Mari A (2009) J Alloys Compd 476:705
16. Ebrahimi F, Li HQ (2007) J Mater Sci 42:1444. doi:10.1007/s10853-006-0969-8
17. Herzer G (1990) IEEE Trans Magn 26:1397
18. Ngo DT, Mahmud MS, Nguyen HH, Duong HG, Nguyen QH, Vitie SM, Nguyen C (2010) J Magn Magn Mater 322:342
19. Liu HS, Du YW, Miao XX, Han K, Shen XP, Bu WK (2008) Rare Met 27:545
20. Xiong XY, Finlayson TR, Muddle BC (2003) J Mater Sci 38:1161. doi:10.1023/A:1022833031311
21. DeGraef M, McHenry ME (2007) Structure of materials: an introduction to crystallography, diffraction and symmetry. Cambridge University Press, Cambridge, p 318
22. Liang XB, Kulik T, Ferenc J, Xu BS (2007) J Magn Magn Mater 308:227
23. Ma XH, Wang Z, Han XT, Yin X, Wang BW (2007) Mater Sci Eng A 448:216
24. Han YM, Wang Z, Che XH, Chen XG, Li WR, Li YL (2009) Mater Sci Eng B 156:57
25. Zhang YR, Ramanujan RV (2006) J Mater Sci 41:5292. doi:10.1007/s10853-006-0263-9
26. Niu YC, Bia XF, Wang WM (2007) J Alloys Compd 433:296
27. Makino A, Bitoh T, Inoue A, Masumoto T (2003) Scripta Mater 48:869